Visnyk NTUU KPI Seriia – Radiotekhnika Radioaparatobuduvannia, 2023, Iss. 92, pp. 84–95

UDC 620.179.147

Automated Precision Amplitudes and Phases Measurement of Polyharmonic Eddy Current Signals of Non-destructive Testing

Bazhenov V. G.[1], *Kalenychenko Yu. O.*[1], *Ratsebarskiy S. S.*[1], *Gloinik K. A.*[2]

[1]National Technical University of Ukraine "Igor Sikorsky Kyiv Polytechnic Institute", Kyiv, Ukraine
[2]«LUXOFT-UKRAINE, LLC», Kyiv, Ukraine

E-mail: *yuriykalenychenko@gmail.com*

The development of electronic systems like Field-Programmable Gate Array (FPGA) made them available for mass commercial use. This created conditions for the development and application of software and technical tools implemented on FPGA algorithms for fast processing of digital signals. Such solutions, in turn, opened up new opportunities for the spread of multi-frequency eddy current systems (MFEC) for non-destructive testing (NDT) in the form of systems for simultaneous processing of digital signals of different frequencies, which allows MFEC to effectively compete with pulsed eddy current systems (PEC). This work presents a new algorithm for accurate digital measurement of the MFEC amplitude and phase of harmonic components of polyharmonic signals, which is implemented in hardware and software on FPGA. The measurement of the amplitude and phase of harmonic components is based on the method of orthogonal processing of digital signals, to increase the accuracy of which the necessity of fulfilling the condition of multiplicity of the sampling sequence to the size of the digital signal period has been proved. Compliance with this condition is achieved by adjusting the length of the sampling sequence, which in the proposed algorithm is performed before orthogonal processing. The influence of inaccuracy in setting the length of the sampling sequence on the size of measurement errors when determining the amplitude and phase of the harmonic components of the signal is simulated. As a result of the simulation, it was established that when the multiplicity condition is met, the measurement error significantly decreases, which indicates the high efficiency of our algorithm. The achieved accuracy of measuring the amplitude of harmonic components and the phase of polyharmonic signals due to the given hardware and software implementation of the algorithm makes it possible to create inexpensive, compact, scalable automated digital systems, the measurement data of which can be used both to determine the individual characteristics of the object and to reconstruct three-dimensional images, i.e. in tomographic systems.

Keywords: algorithm; phase measurement; orthogonal method; measurement error; non-destructive testing; eddy current; multifrequency signal; polyharmonic signal; harmonics

DOI: 10.20535/RADAP.2023.92.84-95

Introduction

An important condition for the automation of eddy current (EC) non-destructive testing operations is the reliable interpretation of the results of scanning of controlled objects, which is achieved by controlling the parameters of the excitation signals, such as amplitude and frequency, followed by appropriate processing and control of the parameters of the response signals. The pulsed eddy current (PEC) systems non-destructive testing (NDT) method is the most common due to the wide frequency spectrum of the pulse signal due to its pulse shape, and the test result is usually obtained by processing the data through the Fourier transform or a similar transformation in the frequency-time domain followed by intelligent interpretation. An alternative to the PEC method is multi-frequency eddy current (MFEC) systems methods of non-destructive testing, when scanning an object is performed using signals of specifically selected frequency values [1–3] or polyharmonic signals [4–6]. MFEC have not become as widespread as PEC, which is due to the complexity of simultaneously supplying the wide frequency spectrum to the channel, but recently their efficiency has improved due to the introduction of digital processing, including signal synthesis [1, 7, 8]. Thus, the use of modern Field-Programmable Gate Array (FPGA)-based systems provides automatic simultaneous multi-channel processing of signals of different frequencies in a selected range with a specified step, which allows reconstructing defective images on maps of scan results [1], or increasing the speed of parallel processing of multi-frequency signals while maintaining a high signal-to-noise ratio [9]. The use of

an artificial neural network with a radial basis function, which was used to process impedances at five frequencies, was demonstrated for fit/unfit classification [2].

The new approach, based on the use of EC giant magnetoresistive algorithms for converting sensor data and multidimensional optimization procedures, allows to reduce the influence of MFEC artifacts and strengthen the influence of defect information [3]. At certain values of the frequencies of the excitation signal, the inductance of the sensor practically does not depend on the lift-off effect, and inverse solver algorithms are proposed for the automated selection of such frequencies [10]. Also, the connection of the MFEC frequencies with the real component of the coil inductance makes it possible to display the seam zones, and as a result, to determine the microstructures of these zones with high sensitivity [11, 12]. The simultaneous use of four frequencies and the automation of the movement of the sensors provides fast scanning of surface damage of cellular panels of the aircraft with a quality that exceeds optical 3-dimensional scanning [13]. Multi-frequency signals in the frequency range of $1 \div 1000$ kHz are used to determine the microstructure of steel rails, namely the depth of decarburization of steel as a result of heat treatment [14]. In general, when using automated methods and algorithms for pattern recognition, the efficiency of MFEC systems is not inferior to PEC systems, which brings them to the level of tomographic systems [15]. However, the traditional key elements of automation are the intelligent processing of the measured values of the signal amplitude by complex algorithms.

The improvement of MFEC methods expands their capabilities not only in the parameterization of defects, but also in determining changes in the structure of materials. The study of physical phenomena in solid state physics, in electromagnetic theory, led to the discovery of new, more informative features in the use of EC methods, which are related to the structure of the studied materials. For example, if, as mentioned above, only the values of the amplitudes of certain frequencies are determined in the MFEC, then it is proposed to determine the phase characteristics of higher harmonics in addition to the amplitudes, the values of which, as experimental results show, are more informative. Traditionally, the procedure for measurement of higher harmonics is not simple, it requires the use of filters, in addition, a fleet of vector voltmeters or special phase meters is required for simultaneous measurement, and to build a family of graphs with such primary results, the control time of one component can be measured in hours. Thus, the use of phase characteristics of polyharmonic and multifrequency signals in eddy current non-destructive testing was limited or impossible. To overcome the above limitations of MFEC, we proposed a new algorithm for accurate digital measurement of the amplitude and phase of the harmonic components of a polyharmonic signal. This algorithm is hardware and software implemented on FPGA and is based on the features of MFEC excitation signal synthesis and orthogonal processing of response signals, which are discussed below.

1 Method

To determine the amplitude and phase of the harmonic components of the analog response signal, which are measured from the output of the EC probe, we used the orthogonal method of their processing [16, 17]. It is generally known that:

$$\begin{aligned} \sin(\omega t+\varphi)\cdot\sin(\omega t) &= \frac{1}{2}\cos(\varphi)-\frac{1}{2}\cos(2\omega t+\varphi), \\ \sin(\omega t+\varphi)\cdot\cos(\omega t) &= \frac{1}{2}\sin(\varphi)+\frac{1}{2}\sin(2\omega t+\varphi). \end{aligned} \tag{1}$$

It follows from expression (1) that after multiplying two signals of the same frequency, the result will have a constant component $\frac{1}{2}\cos(\varphi)$ or $\frac{1}{2}\sin(\varphi)$ and variable harmonic component $\frac{1}{2}\cos(2\omega t+\varphi)$ or $\frac{1}{2}\sin(2\omega t+\varphi)$. A sine wave is a harmonic signal whose signal properties are:

$$\begin{aligned} \int_0^{N_0 T} \sin(\omega t)dt = 0, \\ \int_0^{N_0 T} \cos(\omega t)dt = 0, \end{aligned} \tag{2}$$

where T is the period of the signal, $N_0 = 1, 2, 3, 4\ldots$ ($N_0 \in \mathbb{Z}^+$) is the number of periods.

The result of integration depends only on the constant component, since the integration of all harmonic components by (2) is zero in the case of compliance with the condition that the number of periods N_0 belongs to the positive set of integers, $\mathbb{Z}^+$. Determination of constant components will allow calculation of both amplitudes and phases of signals.

On the basis of the above, a digital method and system for determining the structure of the material of the object was proposed and patented in Ukraine under the number 125416. System and digital method implement the MFEC algorithm, the functional scheme of which is presented in Fig. 1.

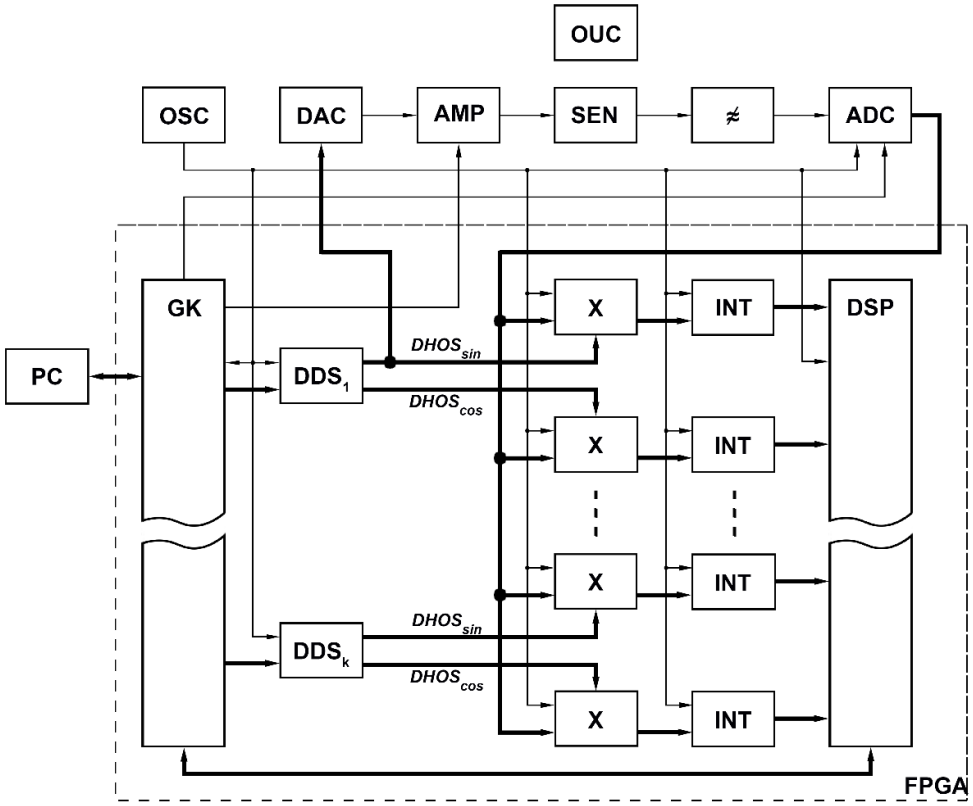

Fig. 1. The functional schematic of the system for determining the structure of the material consists of the following blocks: PC – personal computer, OSC – oscillator, GK – control unit, DAC – digital-to-analogue converter, DDSk – direct digital synthesizer of k-harmonic frequency, AMP – adjustable power amplifier, SEN – sensor, X – digital multipliers, INT – digital integrators, ADC – analog-to-digital converter, DSP – digital signal processor unit

The algorithm of the proposed system is as follows: at the command of the control unit (GK), which is pre-programmed by the computer (PC), at the output of the first digital synthesizer of the frequency of digital signals (DDS1), the frequency of the 1st harmonic f is set, which is defined as:

$$f = N_0 f_{sr}/n_l, \tag{3}$$

where N_0 is the digital code of frequency f; f_{sr} – frequency of the synchronous generator (OSC); n_l – length of the look-up table (LUT) of the sine values of the digital synthesizer of sinusoidal signals (in our case, $n_l = 2^{28}$).

Frequency from DDS1 is set in the form of an orthogonal set of numerical samples $DHOS_{sin}(x)$, and $DHOS_{cos}(x)$ with period $T_p = n_l/f_0$. This set of samples $DHOS_{sin}(x)$, from corresponding output of DDS1, using DAC is transformed into a highly accurate sinusoidal analog signal of excitation of the primary winding of the sensor with a minimum harmonic coefficient, the phase of which will be uniquely determined by the digital output $DHOS_{sin}(x)$ of DDS1. A stepwise change in the power of the sensor excitation in the process of studying the object is performed using a controlled unit (GK) according to a given program of a power amplifier (AMP). It is known that when metal objects are excited by an electromagnetic field, eddy currents arise not only with the frequency of the first harmonic, but with the frequencies of higher harmonics [6,16], which are perceived by the measuring winding of the sensor (SEN) and through the anti-aliasing filter enter the input of the analog-to-digital converter (ADC). Sample sets $DRS(x)$ from ADC get to the corresponding information inputs of digital multipliers (X) the second inputs of which receive sets of sample reference orthogonal signals $DHOS_{sin}(x)$, and $DHOS_{cos}(x)$ from the corresponding frequency synthesizers (DDS).

That is, there is a multiplication of samples of the digital response signal presented in the form of sequences $DRS(x)$, formed by analog-digital transformations, with specially formed reference digital harmonic orthogonal signals, which are sequences of samples with a known amplitude and phase, the frequency of which is equal to the frequency of the harmonics under study, and their length coincides with

the length of the digital response signal:

$$\begin{aligned} s_{cos_k}(x) &= DRS(x) \cdot DHOS_{sin}(x), \\ s_{sin_k}(x) &= DRS(x) \cdot DHOS_{cos}(x), \end{aligned} \tag{4}$$

where k is a harmonic number, $s_{cos_k}(x)$, $s_{sin_k}(x)$ – intermediate signals, $DRS(x)$ – digital response signal, $DHOS_{cos}(x)$, $DHOS_{sin}(x)$ – digital harmonic reference orthogonal signals, x – sample number in the sequence, $0 \leq x < M$, $x = 0, 1, 2, 3, 4\ldots$, and M – its length. The main principle is that all these harmonics, regardless of the frequency difference, are in phase, because the DDS, ADC, DAC, DSP block synchronization signals are generated from the same source of the OSC generator. Thus, at the outputs of each pair of multipliers, we will receive information about the real and imaginary part of each harmonic, that is, we will perform quadrature demodulation of the received harmonics. Given that we are working with digital signals, instead of analog integration to get rid of the variable components, we will use numerical integration, also known as averaging, of expression (4), which will look like this:

$$\begin{aligned} \frac{1}{M_{IS}} \sum_{x=0}^{M_{IS}-1} s_{cos_k}(x) &= \frac{1}{2} A_k cos(\varphi_k), \\ \frac{1}{M_{IS}} \sum_{x=0}^{M_{IS}-1} s_{sin_k}(x) &= \frac{1}{2} A_k sin(\varphi_k), \\ M_{IS} &= m \cdot n, \end{aligned} \tag{5}$$

where M_{IS} is the length of the sequence of the intermediate signal, and m is the number of its periods with a fractional part, or $m \in \mathbb{R}^+$, $n = \frac{f_{sr}}{f}$ is the number of points in the period of the intermediate signal, where f_{sr} is the clock signal frequency OSC, f is the excitation signal frequency, A_k is amplitude of the k-th harmonic and φ_k is phase of the k-th harmonic of the digital response signal.

From expressions (5), using the function of the two-argument arctangent, we obtain the value of the phase of the k-th harmonic of the digital response signal:

$$\begin{aligned} \varphi_k &= atan2\left(\frac{\frac{1}{M_{IS}}\sum_{x=0}^{M_{IS}-1} s_{cos_k}(x)}{\frac{1}{M_{IS}}\sum_{x=0}^{M_{IS}-1} s_{sin_k}(x)}\right) = \\ &= atan2\left(\frac{\frac{1}{M_{IS}}\sum_{x=0}^{M_{IS}-1} DRS(x) \cdot DHOS_{cos}(x)}{\frac{1}{M_{IS}}\sum_{x=0}^{M_{IS}-1} DRS(x) \cdot DHOS_{sin}(x)}\right). \end{aligned} \tag{6}$$

Similarly, we obtain the value of the amplitude of the k-th harmonic of the digital response signal:

$$\begin{aligned} A_k &= 2\sqrt{\left(\frac{1}{M_{IS}} \sum_{x=0}^{M_{IS}-1} s_{cos_k}(x)\right)^2 + \left(\frac{1}{M_{IS}} \sum_{x=0}^{M_{IS}-1} s_{sin_k}(x)\right)^2} = \\ &2\sqrt{\left(\frac{1}{M_{IS}} \sum_{x=0}^{M_{IS}-1} DRS(x) \cdot DHOS_{cos}(x)\right)^2 + \left(\frac{1}{M_{IS}} \sum_{x=0}^{M_{IS}-1} DRS(x) \cdot DHOS_{sin}(x)\right)^2}. \end{aligned} \tag{7}$$

The given expressions (6), (7) are synchronously implemented in the DSP block for each harmonic, and the received values of amplitudes and phases are transmitted to the PC via the high-speed Ethernet cable network. Then, according to the GK command, the next step change in the AMP gain coefficient occurs and the sensor is excited again, and at the end of transitional process a new similar cycle of measurement begins, and the accumulation of the data array for processing begins with a sample that corresponds to the frontal zero transition. The number of cycles of step voltage change, the amplitude and range of voltage change, as well as the frequency of the test signal are determined by the operator before the beginning of the research. After the research is completed, families of graphs are automatically built according to the specified protocols Fig. 2.

Obviously, to comply with the condition of the signal number of periods N_0 to the set of positive integer $\mathbb{Z}^+$, the sequence length of the intermediate signal M_{IS} must be a multiple of the digital response signal period T_{DRS}, which can be achieved by algorithmically setting the sequence length M_{IS} of the intermediate signal.

2 Modeling

To assess the effect of inaccuracy in establishing the length of the sequence M_{IS} on the size of errors in determining the amplitude and phase of harmonic components, we investigated the relationship between the fractional part of the number of periods N in the digital response signal, which is called the incompleteness of the integration interval, and the mean absolute error of the amplitude and phase.

The simulation was performed using a Monte Carlo simulation in the MATLAB software package [18]. Simulation characteristics: 25 thousand cycles, step 1% of the integration interval incompleteness, whole periods 39. Simulations with $1, 5, 10$ thousand cycles and steps $0.5\%, 2\%, 5\%$ of the integration interval incompleteness at the whole number of 8 and 15 periods were also performed.

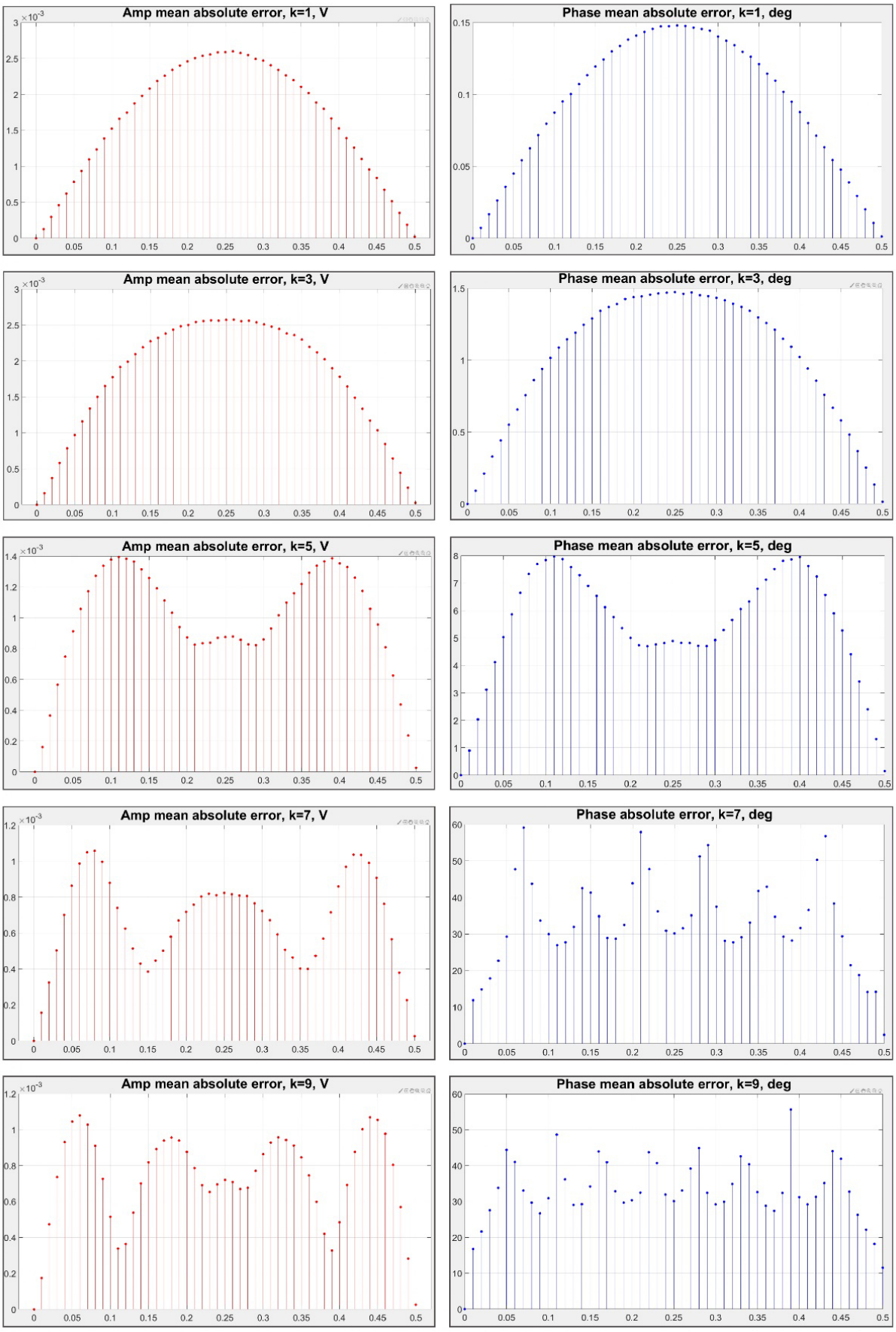

Fig. 2. Dependence of the mean absolute error on the incompleteness of the integration interval: first line — harmonic $k = 1$, amplitude and phase; second line — harmonic $k = 3$, amplitude and phase; third line — harmonic $k = 5$, amplitude and phase; fourth line — harmonic $k = 7$, amplitude and phase; fifth line — harmonic $k = 9$, amplitude and phase

To artificially introduce the incompleteness of the integration interval during the simulation, formulas (5) were changed as follows:

$$\frac{1}{2}A_k cos(\varphi_k) = \frac{1}{M_0 + j}\sum_{x=0}^{M_0+j-1} DRS(x) \cdot DHOS_{cos}(x), \tag{8}$$

where M_0 is the length of the sequence of the intermediate signal, a multiple of the digital response signal period length, j is the number of excess M_{IS} sequence points to M_0.

Formula (8) shows the method of obtaining one of the intermediate results of the calculation, the average value of the sequence used to calculate the values of the selected harmonic amplitude and phase. Figure 3 presents the results of modeling the dependence of the mean absolute error on the incompleteness of the integration interval for odd harmonics up to and including the ninth. Here, the X axis is the value of $\frac{jf}{f_{sr}}$, or the incompleteness of the integration interval, and the Y axis is the modulus of the mean absolute error in volts for the amplitude $|\Delta A|$ and in degrees for the phase $|\Delta\varphi|$. It is observed that for all harmonics the error in amplitude and phase is minimal at points 0 and 1, according to the simulation results it is less than the error of the uncontrolled signal by 5 orders of magnitude. As the number of harmonics k increases, the chaotic error increases in amplitude and phase, while the absolute size of the error in amplitude almost does not change, and in phase increases significantly.

3 Algorithm

To comply with the condition of the integer number of periods, we have proposed the following algorithm, which is implemented as follows (Fig. 4). First, the excitation signal frequency is selected so that it is defined as the clock signal frequency divided by the positive integer n_0 (the nearest smaller positive integer of n), if it does not correspond to the set frequency. Then the number of periods m in the sequence of length M_{IS} is adjusted, which should be determined by a positive integer m_0 (the nearest smaller positive integer of m), and accordingly, the length of the sequence M_{IS} is reduced to $M_0 = m_0 \cdot n_0$.

Response signal sampling is provided using 14-bit ADCs with the maximum sampling rate f_{sr} of 125 MHz.

It is known that the frequency of the output signal of the sensor excitation is formed by the DDS1 synthesizer and is determined according to the expression (3).

Due to discrete nature of the frequency tuning, frequency f can differ from f_s (integer N_0 is a frequency code and determines amount of phase steps $ph = n_l/f_{sr}$). If $N_{0s} = f_s \cdot n_l/f_0$ is not integer, then frequency of output excitation signal f_s is corrected in a way so that it is defined as the clock frequency of the signal multiplied by a positive integer N_0 (closest lesser integer of N_{0s}), if it does not correspond to set frequency.

Example: set frequency $f_s = 1000$ Hz, $n_l = 2^{28}$, $f_{sr} = 125000000$ Hz. If:

$$N_{0s} = f_s \cdot \frac{n_l}{f_{sr}} = 1000 \cdot 2.1474836 = 2147.4836. \tag{9}$$

This number can only be integer, so we choose nearest lesser integer $N_0 = 2147$ – frequency code. Then

$$f = N_0 \cdot \frac{f_{sr}}{n_l} = \frac{2147}{2.1474836} = 999.77 \text{ Hz}. \tag{10}$$

Error is 0.23 Hz. Error versus set frequency plot is presented at Fig. 3. It is clear that error depends on set frequency and can be up to 0.46 Hz.

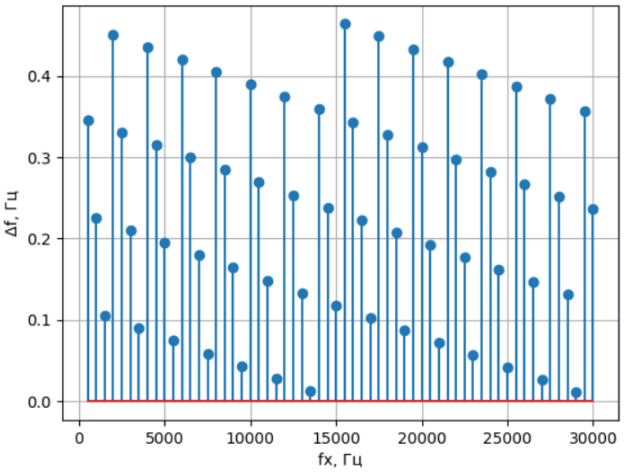

Fig. 3. Error versus set frequency plot

After that, looking at an algorithm on Fig. 4, we determine number of periods m of frequency f_{sr} in a single period of excitation frequency, that must be a positive integer m_0:

$$m = \frac{f_{sr}}{f}. \tag{11}$$

If m is not integer, then the length of sample sequence M is changed so that $M_0 = m_0 \cdot n$.

On the last step of algorithm, presented on Fig. 4, we propose to choose frequency code N equal to 2^i which will ensure that frequency set error will be eliminated and the length of sequence M will always be an integer multiple of m, eliminating error presented on Fig. 3.

Example for frequency 1000 Hz: $f = N_0 \cdot \frac{f_{sr}}{n_l}$ we choose $N_{02} = 2048 = 2^{11}$, as closest to $N_0 = 2147$, then $f = 2^{11} \cdot \frac{125 \cdot 10^6}{2^{28}} = \frac{125 \cdot 10^6}{2^{17}}$, $n_0 = \frac{f_{sr}}{f} = \frac{125 \cdot 10^6 \cdot 2^{17}}{125 \cdot 10^6} = 2^{17}$.

It is worth noting that despite all positives, the number of available frequencies reduces dramatically. On a range, depicted on Fig. 3, there are only 7 of these frequencies.

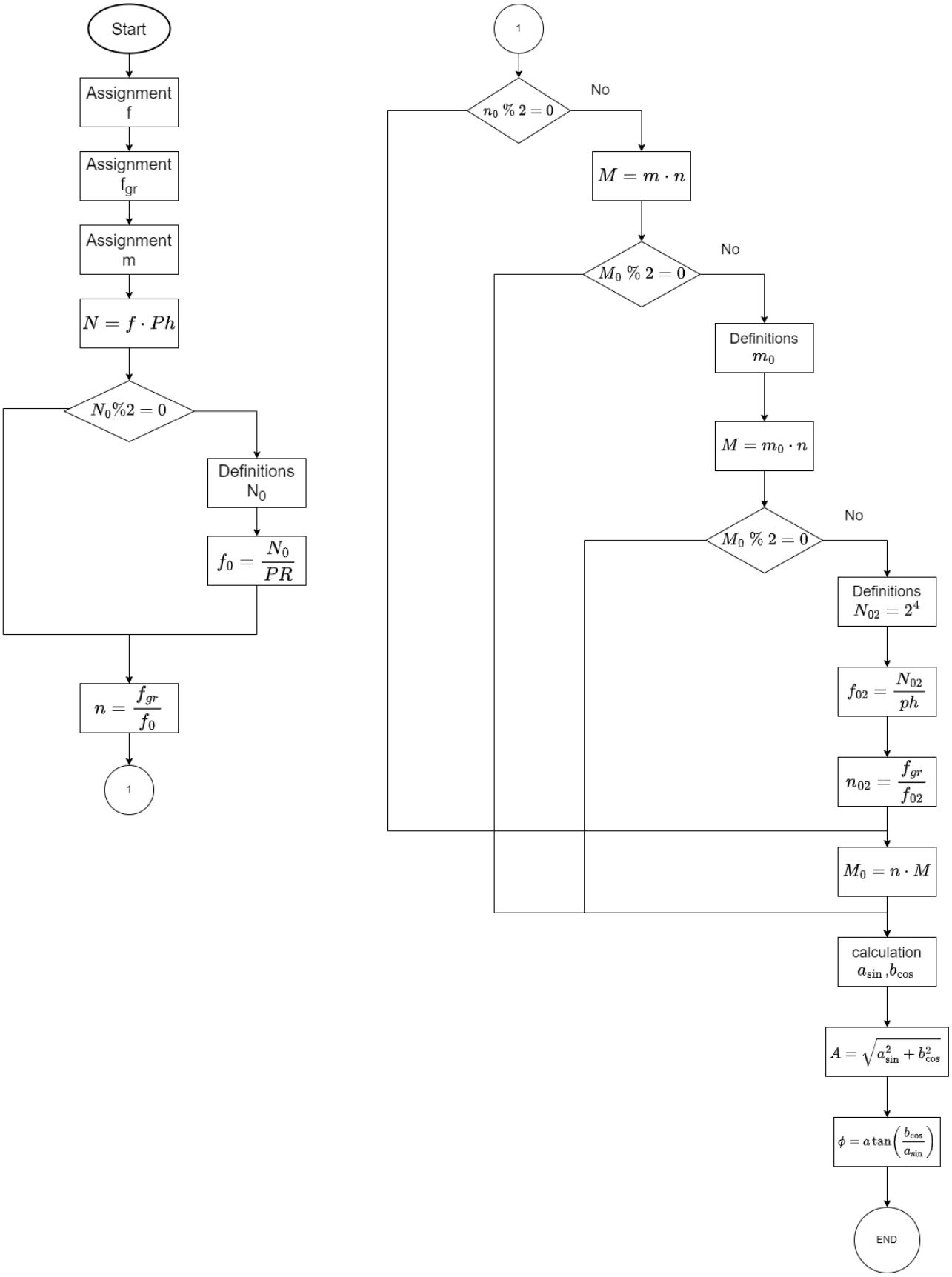

Fig. 4. Algorithm for precise determination of amplitude and phase

4 Results of experimental studies

The plots presented in Fig. 5 show one of the options for presenting information (protocols) for the investigation of a transformer steel plate, using a working model of a multi-frequency eddy current system developed by the authors (or an eddy current system based on higher harmonics [16]). The plots on Fig. 5 clearly demonstrate the ambiguity of the physical processes that occur in the sample under study with an equal step change in the magnetizing field, we observe very interesting anomalies in the changes in the amplitudes and especially the phases of the higher harmonics, which are not at all similar to linear ones. Moreover, each metal sample has its own set of given pictures depending on the type of material under study, chemical composition, hardening conditions, fatigue, and defects in the material. The entire measurement process is automated. One second is required to obtain measurement results at one point. It took about one minute to obtain the given family of graphs (36 points). Each harmonic carries information about the physical processes in the material when the magnetization power changes, it requires a lot of time and a very high qualification from the operator to evaluate the obtained results and make a decision, but considering that all the information presented on the graphs is digital and fully computerized, then the system can be equipped with artificial intelligence for instant decision making. The authors do not know of such automatic digital systems in the world.

A photo of the working model of the multi-frequency eddy current system is presented in Fig. 6.

5 Measurement errors of higher harmonics amplitudes and phases

In the given plots Fig. 7, Fig. 8, Fig. 9, Fig. 10, Fig. 11 we present a 100 point series of measurements of amplitudes and phases of the measured harmonics of the samples under constant magnetization power (the voltage at the output of the measuring winding of the sensor is about 200 mV). The measurements were performed for very small signal amplitudes, because the results of real measurements are given to demonstrate the possibilities of such measurements of both amplitude and phase, in which the amplitudes of the harmonics are much smaller (can be several hundreds of times smaller) than the amplitude of the first harmonic, which is less informative but is also present in this informative (multi-frequency) response signal. A 14-bit ADC with a sampling frequency of 125 MHz is used.

On the graphs, the zone of deviation of the results at the 3σ level is marked with a red line (where σ is the mean squared error calculated for this array of measurements). Here, the X axis is the measurement number; Y axis is the value of the amplitude in volts and for the phase in degrees.

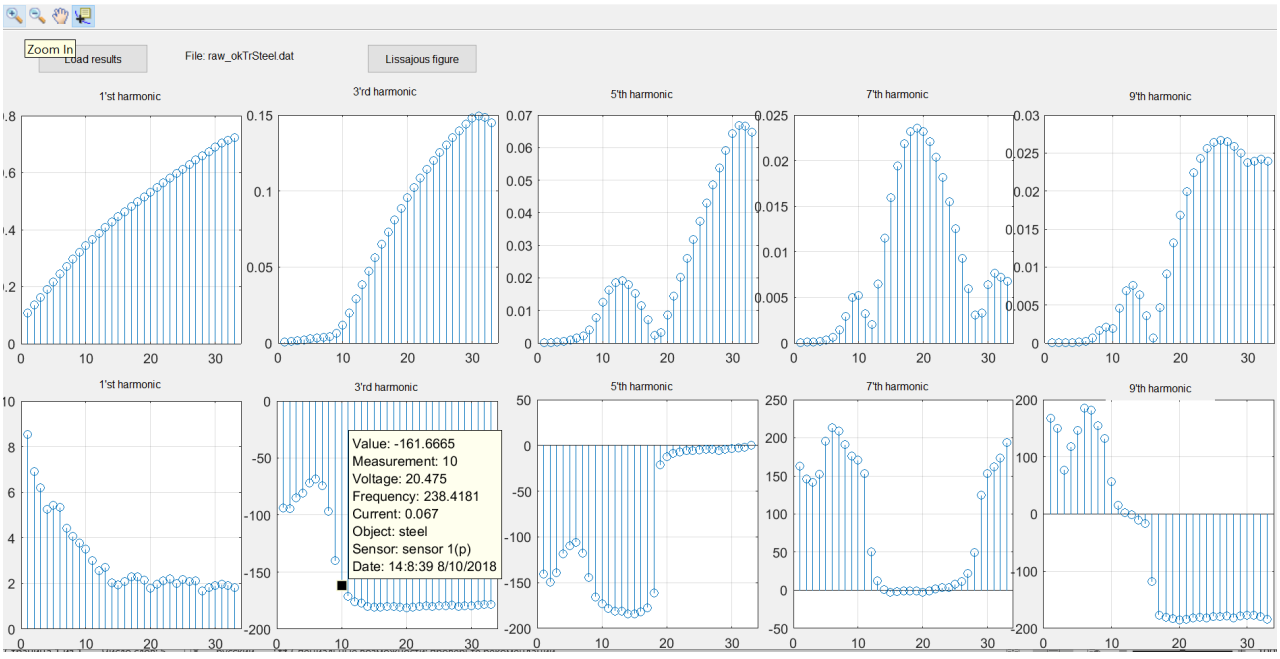

Fig. 5. Graphs of changes in the amplitudes and phases of the harmonics of the response signal during the investigation of the transformer steel plate. The first line is an amplitude change of 1st, 3rd, 5th, 7th and 9th harmonics, and the second line is a phase change of the corresponding harmonics depending on the amplitude (36 equal-step changes) of the excitation signal

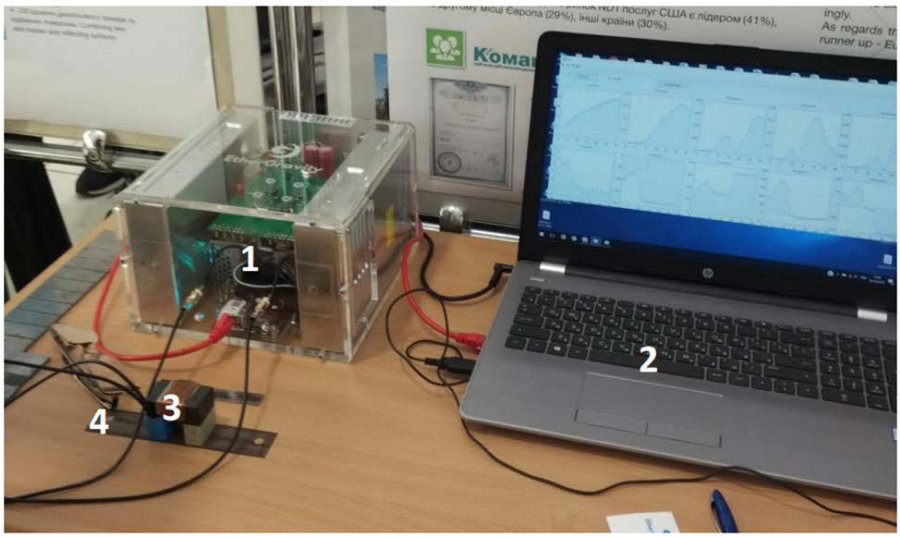

Fig. 6. A working model of a multi-frequency eddy current system: where 1 – the model itself, 2 – a personal computer, 3 – a sensor, 4 – a researched sample of transformer steel

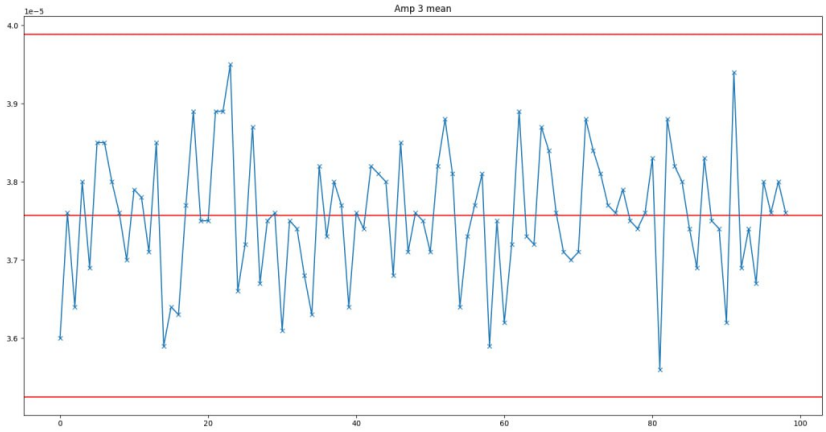

Fig. 7. A plot of 100 measurements of amplitude of 3rd harmonic

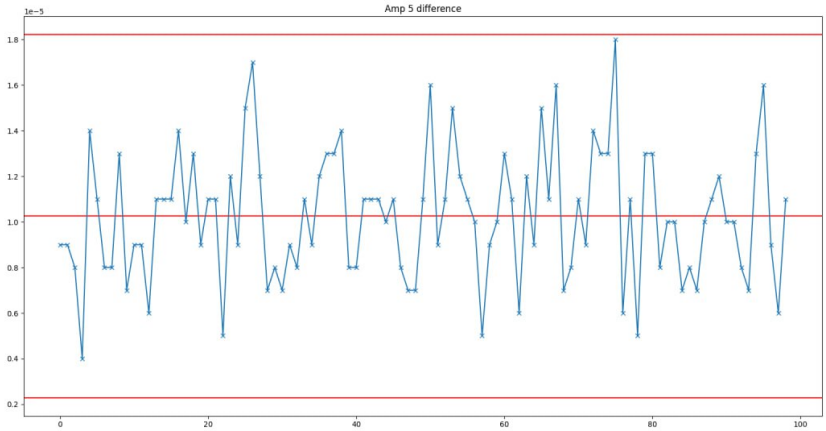

Fig. 8. A plot of 100 measurements of amplitude of 5th harmonic

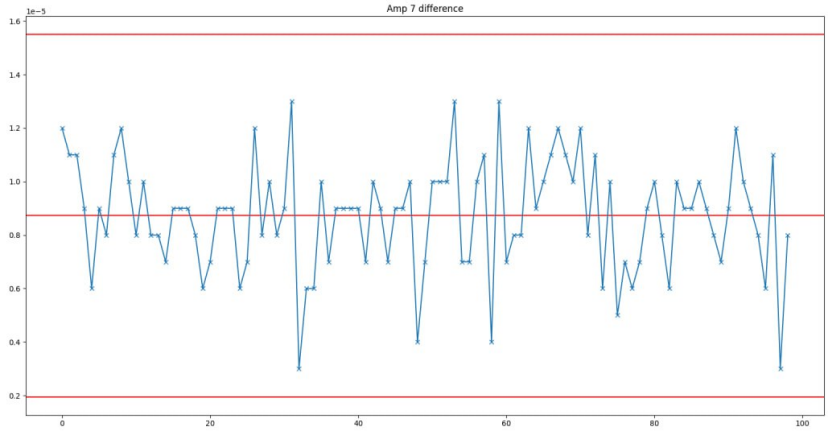

Fig. 9. A plot of 100 measurements of amplitude of 7th harmonic

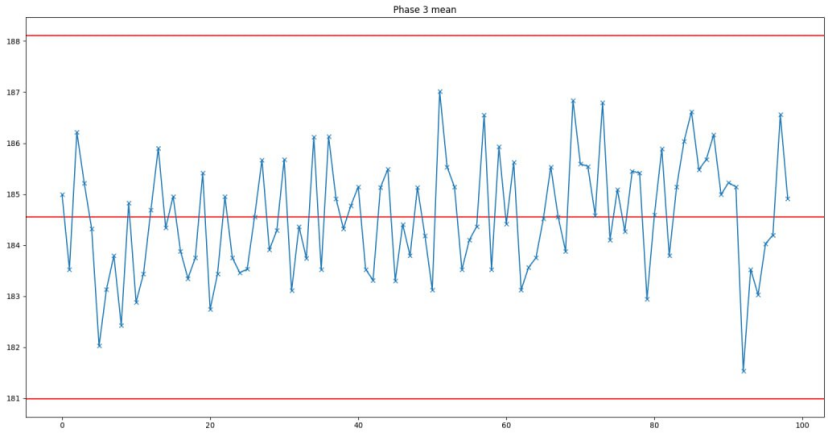

Fig. 10. A plot of 100 measurements of phase of 3rd harmonic

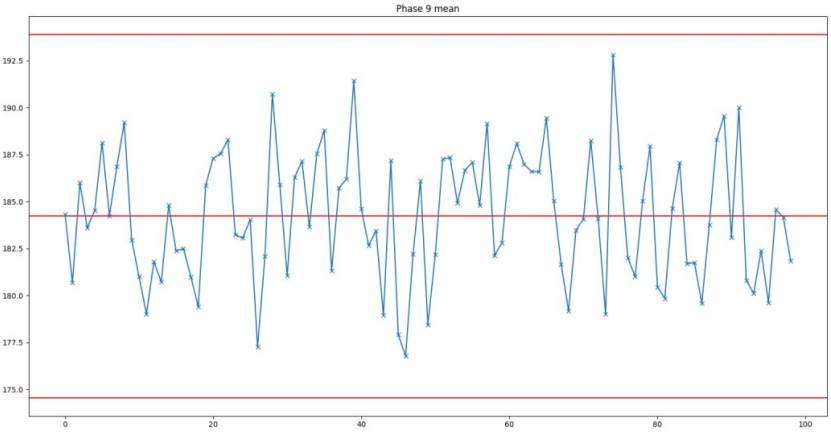

Fig. 11. A plot of 100 measurements of phase of 9th harmonic

The given graphs of measurements with a sufficient length of the measurement sequence, as shown by the experiments, which can be evidenced by Fig. 5, allow the studies above to be performed with high reliability.

Conclusions

The use of FPGAs and precise high frequency ADC made it possible to build a fully digital automatic material control system based on direct measurements (without frequency conversion of the received measurement signal) on a single FPGA chip, made it possible to propose and implement algorithms for measurement and signal processing using one measurement channel, regardless of phase multichannel and multi-frequency measurements, which in turn, made it possible to significantly increase the accuracy of the measurement and use only one expensive precision ADC. Moreover, the system can be reconfigured by software without mechanical changes. For example: you can increase the number of defined harmonics, you can simultaneously determine the parameters of both even and odd harmonics, change the measurement parameters, change the algorithm, change the form of the protocol for automatic registration of research results.

The system is fully digital, automatic, fast-acting (the measurement time at one point is 1 second), therefore the developed control algorithm can be integrated without problems into any automated technological process. A compact digital computer-integrated automated MFEC system was developed and manufactured, which allows determination of the amplitude-phase characteristics of harmonic components of polyharmonic signals (see Fig. 6) and obtain the final result in the form of a family of graphs or maps of reconstructed images from the scanned plane without using a fleet of measuring devices. A large array of digital data obtained during the measurement of amplitude-phase-amplitude characteristics can be additionally processed using artificial intelligence, which at the same time will significantly increase the probability of control and significantly speed up the time of assessment of the state of the controlled object. To date, there are no analogues of similar systems in the world. Part of the research on the introduction of artificial intelligence into the system is carried out at the expense of a European grant under the Framework Program for Research and Innovation Horizon 2020 of the European Commission, the second open competition «DIH-World — Accelerating the deployment and maturity of DIH for the digitalization of European SMEs», Grant Agreement № 952176, received by the authors of the project.

The work investigates the possible causes of measurement errors, based on the research, algorithms for optimal system operation modes with the possibility of maximum suppression of these errors are proposed. A model of the working system was developed and manufactured, as well as the graphs of experimental studies of samples and graphs of experimental studies of errors confirm the high reliability and efficiency of the proposed and analyzed work algorithms.

References

[1] Avila J.R.S., Chen Z., Xu H. and Yin W. (2018). A multi-frequency NDT system for imaging and detection of cracks. *2018 IEEE International Symposium on Circuits and Systems (ISCAS)*, pp. 1-4. doi:10.1109/ISCAS.2018.8351849.

[2] Martínez-Martínez, V., Garcia-Martin, J., Gomez-Gil, J. (2017). RBF-Neural Network Applied to the Quality Classification of Tempered 100Cr6 Steel Cams by the Multi-Frequency Nondestructive Eddy Current Testing. *Metals*, Vol. 7(10), 385. doi:10.3390/met7100385.

[3] Karpenko O., Efremov A., Ye C., Udpa L. (2020). Multi-frequency fusion algorithm for detection of defects under fasteners with EC-GMR probe data. *NDT & E International*, Vol. 110, 102227. doi:10.1016/j.ndteint.2020.102227.

[4] Svatoš J., Pospíšil T., Vedral J. (2018). Application of poly-harmonic signals to eddy-current metal detectors and to advanced classification of metals. *Metrol, Meas. Syst.*, Vol. 25, No. 2, pp. 387–402. DOI: 10.24425/119564.

[5] Svatoš, J. (2016). Single-tone and Polyharmonic Eddy Current Metal Detection and Non-Destructive Testing Education Software. *Journal of Physics: Conference Series*, Vol. 772, 012052. DOI:10.1088/1742-6596/772/1/012052.

[6] Kalenychenko Yu., Bazhenov V., Kalenychenko A., Koval V., Ratsebarskiy S. (2019). Determination of Mechanical Properties of Paramagnetic Materials by Multi-frequency Method. *International Journal "NDT Days"*, Vol. II, Iss. 4, pp. 406-416.

[7] Kuts Y., Protasov A., Lysenko I., Dugin O., Bliznuk O. and Uchanin V. (2017). Using Multidifferential Transducer for Pulsed Eddy Current Object Inspection. *2017 IEEE First Ukraine Conference on Electrical and Computer Engineering (UKRCON)*, pp. 826-829.

[8] Bazhenov V., Protasov A. and Gloinik K. (2017). Increasing of operation speed of digital eddy current defectoscopes based on frequency synthesizer. *2017 IEEE Microwaves, Radar and Remote Sensing Symposium (MRRS)*, pp. 155-158. DOI: 10.1109/MRRS.2017.8075051.

[9] Chen Z., Salas-Avlia J.R., Tao Y., Yin W., Zhao Q., and Zhang Z. (2020). A novel hybrid serial/parallel multi-frequency measurement method for impedance analysis in eddy current testing. *Review of Scientific Instruments*, Vol. 91, 024703. doi:10.1063/1.5130734.

[10] Lu M., Meng X., Huang R., Chen L., Peyton A., Yin W. (2021). Lift-off invariant inductance of steels in multi-frequency eddy-current testing. *NDT & E International*, Vol. 121, 102458. doi:10.1016/j.ndteint.2021.102458.

[11] Xu, H., Lu, M., Avila, J. R. Salas, et al. (2019). Imaging a weld cross-section using a novel frequency feature in multi-frequency eddy current testing. *Non-Destructive Testing and Condition Monitoring*, Vol. 61, Iss. 12, pp. 738-743(6). doi:10.1784/insi.2019.61.12.738.

[12] Zhou Z., Qin M., Xie Y., Tan J. and Bao H. (2020). Experimental Study of Microstructures in Bias Weld of Coiled Tubing Steel Strip With Multi-Frequency Eddy Current Testing. *IEEE Access*, Vol. 8, pp. 48241-48251. doi:10.1109/ACCESS.2020.2979414.

[13] Reyno T., Underhill P. R., Krause T. W., Marsden C., and Wowk D. (2017). Surface Profiling and Core Evaluation of Aluminum Honeycomb Sandwich Aircraft Panels Using Multi-Frequency Eddy Current Testing. *Sensors*, Vol. 17(9), 2114. doi:10.3390/s17092114.

[14] Zhu W., Yin W., Dewey S., Hunt P., Davis C. L., Peyton A. J. (2017). Modeling and experimental study of a multi-frequency electromagnetic sensor system for rail decarburisation measurement. *NDT & E International*, Vol. 86, pp. 1-6. doi:10.1016/j.ndteint.2016.11.004.

[15] Dingley, G. and Soleimani, M. (2021). Multi-Frequency Magnetic Induction Tomography System and Algorithm for Imaging Metallic Objects. *Sensors*, Vol. 21(11), 3671. doi:10.3390/s21113671.

[16] Dorofeev A. L., Kazamanov Iu. G. (1980). *Electromagnetic defectoscopy*. Moscow: Mashinostroenie, 232 p.

[17] Bohdan H., Bazhenov V. and Protasov A. (2017). Development of a discrete orthogonal method for determining the phase shift between high-frequency radio impulse signals. *IEEE Microwaves, Radar and Remote Sensing Symposium (MRRS)*, pp. 191-194. DOI: 10.1109/MRRS.2017.8075060.

[18] Chopin N., Papaspiliopoulos O. (2020). An Introduction to Sequential Monte Carlo. *Springer*, 402 p. doi:10.1007/978-3-030-47845-2.

Автоматизоване прецизійне вимірювання амплітуд і фаз полігармонійних сигналів вихрострумового неруйнівного контролю

Баженов В. Г., Калениченко Ю. О., Рацебарський С. С., Гльойнік К. А.

Розвиток електронних систем в останні роки, таких як програмовані логічні інтегральні схеми (Field-Programmable Gate Array, FPGA), зробив їх доступними для масової комерційної експлуатації. Це створило умови для розробки і застосування програмно-технічних засобів, реалізованих на FPGA алгоритмах швидкої обробки цифрових сигналів. Такі рішення, в свою чергу, відкрили нові можливості для поширення багаточастотних вихрострумових систем (multi-frequency eddy current systems, MFEC) неруйнівного контролю (non-destructive testing) у вигляді систем одночасної обробки цифрових сигналів різних частот, що дозволяє MFEC ефективно конкурувати з імпульсними вихрострумовими системами (pulsed eddy current systems). У даній роботі представлений новий алгоритм точного цифрового вимірювання амплітуди MFEC і фази гармонічних компонентів полігармонійних сигналів, який реалізований в апаратному і програмному забезпеченні на FPGA. Вимірювання амплітуди і фази гармонійних компонентів базується на методі ортогональної обробки цифрових сигналів, для підвищення точності якого доведена необхідність виконання умови кратності послідовності вибірки до розміру періоду сигналу. Дотримання цієї умови досягається регулюванням довжини послідовності вибірки, яка в запропонованому алгоритмі виконується перед ортогональною обробкою. Змодельовано вплив неточності у встановленні довжини послідовності вибірки на розмір похибок вимірювань при визначенні амплітуди і фази гармонічних компонентів сигналу. В результаті моделювання було встановлено, що при виконанні умови кратності похибка вимірювання значно зменшується, що говорить про високу ефективність роботи нашого алгоритму. Досягнута точність вимірювання амплітуди і фази компонентів полігармонійних сигналів за рахунок заданої апаратно-програмної реалізації алгоритму дозволяє створювати недорогі, компактні, масштабовані автоматизовані цифрові систем, дані вимірювань яких можуть бути використані як для визначення індивідуальних характеристик об'єкта контролю, так і для реконструкції тривимірних зображень, тобто в томографічних системах.

Ключові слова: алгоритм; вимірювання фази; ортогональний метод; похибка вимірювання; неруйнівний контроль; вихрові струми; багаточастотний сигнал; гармоніки